JOURNAL OF MATERIALS SCIENCE 13 (1978) 1901–1906

Mechanical properties of precipitation-strengthened Ni-Al-Cr alloy based on an NiAl intermetallic compound

R. MOSKOVIC*
Department of Metallurgy and Material Science, University of Cambridge, Pembroke Street, Cambridge

Mechanical properties of a ternary alloy Ni–30.3 at. % Al–6.6 at. % Cr have been studied in the temperature range 25 to 1100° C. The material was heat-treated to produce a stable dispersion of incoherent rod-shaped Ni_3Al precipitates, 1 μm in diameter and 20 μm long. The tensile properties were found to be temperature dependent. Below 750° C the material had high strength, low ductility and low strain-rate sensitivity, whilst above 750° C the strength fell, ductility increased and the material became strain-rate sensitive. The room temperature fracture toughness of the single-phase material was 6 MN $m^{-3/2}$ and increased to 50 MN $m^{-3/2}$ in the two-phase material. This can be attributed to the effect of Ni_3Al on crack nucleation and propagation.

1. Introduction

The mechanical properties of NiAl intermetallic compounds have aroused considerable interest in recent years. These properties have been measured as a function of both temperature and composition. It has been shown [1, 2] that polycrystalline NiAl is brittle below 0.45 T_m. Limited ductility has been reported in fine grain sized (50 μm) material [3]. Polycrystalline NiAl is ductile at elevated temperatures but this is accompanied by a rapid decrease in strength [3, 4]. Russell and Edington [5] have shown that, in Ni–36 at. % Al, Ni_3Al precipitates improve the low temperature ductility whilst high strength is maintained up to 700° C. The present study has been undertaken to determine whether the strengthening effect of Ni_3Al precipitates can be maintained above 700° C.

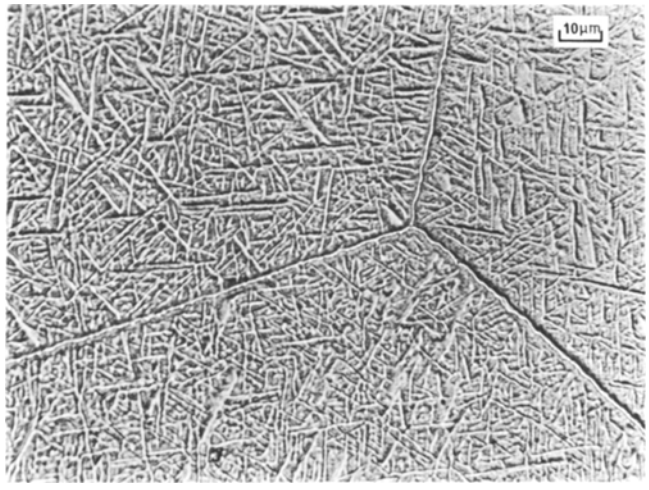

Figure 1 The microstructure of the material aged for two hours at 850° C.

*Present Address: CEGB, Scientific Services Department, Gravesend Laboratory, Canal Road, Gravesend.

2. Experimental procedures

A ternary alloy Ni–30.3 at.% Al–6.6 at.% Cr was prepared by argon arc melting, encapsulation in mild steel and extrusion at 1100° C. The alloy was solution treated at 1300° C for one hour and then aged for two hours at 850° C in argon. This heat treatment produced a 50% volume fraction of incoherent rod-shaped Ni_3Al precipitates which were 1 μm wide and 20 μm long. Fig. 1 shows the microstructure.

Tensile tests were carried out in an argon atmosphere in the temperature range 25 to 1100° C at strain rates of 3.28×10^{-2} sec^{-1} and 3.28×10^{-4} sec^{-1}. Standard Instron specimens (single shoulder) were used. The gauge length was 28.575 mm long with 4.064 mm specimen diameter. Prior to testing the specimens were held in the furnace for 45 min in order to reach a constant temperature. As a result of this temperature equilibration, the volume fraction of the precipitate decreased to 42% at 1000° C and 35% at 1100° C. The precipitate size increased to 25×1.8 μm and 32×2.5 μm, respectively. No microstructural changes were observed during the temperature equilibration at the other testing temperatures.

3. Results

3.1. Tensile testing

The 0.2% proof stress and strain to fracture are shown in Fig. 2. The tensile data for stoichiometric NiAl [4]; compression data for a single phase Ni–43 and 41.6 at.% Al [3]; and compression data for both a single phase Ni–36 at.% Al and a two-phase Ni–38 at.% Al alloy [5] are included for comparison. The precipitation-hardened material is clearly stronger than the single-phase material below 900° C but there is almost no difference above this temperature.

At the lower strain rate, below 750° C specimens failed predominantly by cleavage although up to 10 to 20% of the fracture surface was inter-

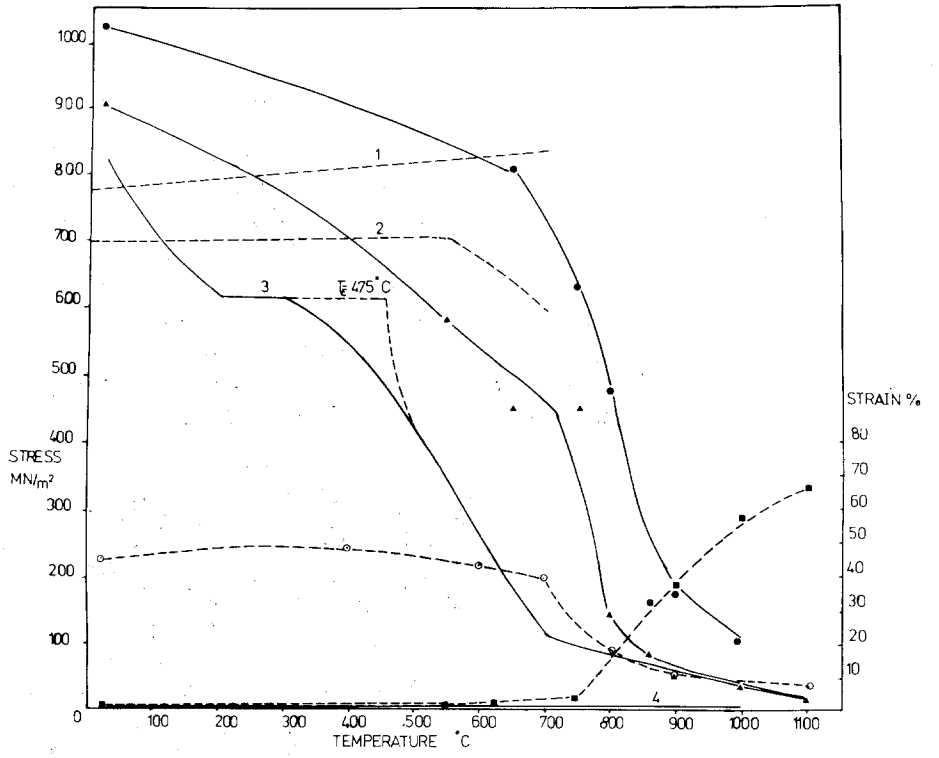

Figure 2 Tensile data for the Ni–30.3 at.% Al, 6.6 at.% Cr alloy compared with the data in the literature for single-phase and two-phase NiAl alloys.
0.2% proof stress
● Ni–30.3 at.% Al, 6.6 at.% Cr; $\dot{\varepsilon} = 3.28 \times 10^{-4}$ sec^{-1}, ▲ Ni–30.3 at.% Al, 6.6 at.% Cr; $\dot{\varepsilon} = 3.28 \times 10^{-4}$ sec^{-1},
1 Ni–36 at.% Al; $\dot{\varepsilon} = 1.2 \times 10^{-3}$ sec^{-1} [5], 2 Ni–38 at.% Al; $\dot{\varepsilon} = 1.2 \times 10^{-3}$ sec^{-1} [5],
3 Ni–43 and 41.6 at.% Al $\dot{\varepsilon} = 2.2 \times 10^{-4}$ sec^{-1} [3], ○ Ni–50 at.% Al; $\dot{\varepsilon} = 1.1 \times 10^{-3}$ sec^{-1} [4].
Strain to failure
4 Ni–30.3 at.% Al, 6.6 at.% Cr; $\dot{\varepsilon} = 3.28 \times 10^{-2}$ sec^{-1}, ■ Ni–30.3 at.% Al, 6.6 at.% Cr; $\dot{\varepsilon} = 3.28 \times 10^{-4}$ sec^{-1}.

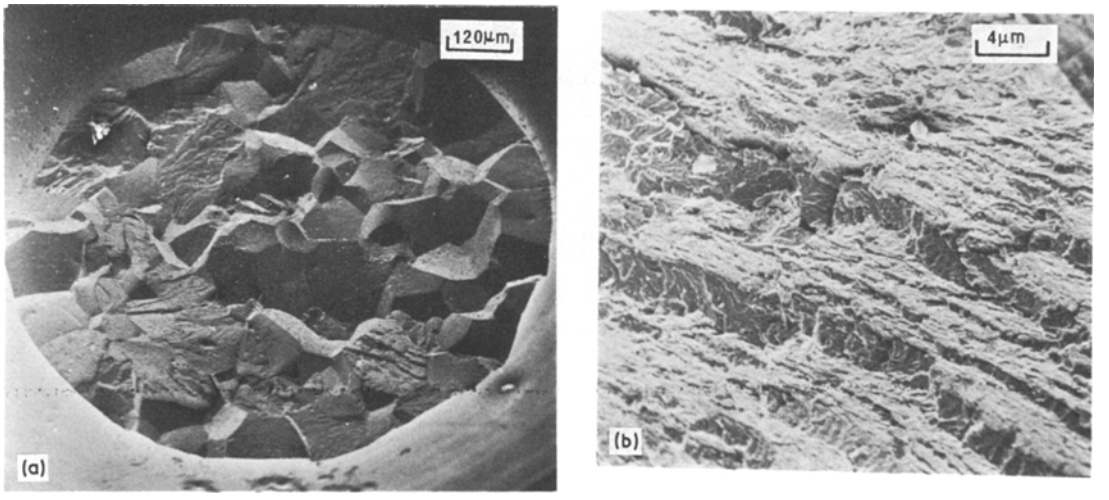

Figure 3 Brittle fracture in a predominantly transgranular (cleavage) mode, (a) overall view, (b) a detailed view of the cleavage steps.

granular. The fracture surface was rough, exhibiting cleavage steps, crack-branching and considerable deformation of the Ni_3Al particles, as shown in Fig. 3. Similar observations were reported by Russell and Edington [5].

In the temperature range 800 to 900° C the grains deformed extensively but there was considerable grain-boundary sliding. There was also significant necking of the specimen during deformation. The Ni_3Al laths and grain-boundary film were destroyed in the necked region and this phase was spheriodized. The fracture was characteristic of the "cup and cone" type (Fig. 4). Above 900° C the deformation was accompanied by extensive grain-boundary sliding at the interface between the Ni_3Al grain-boundary film and the NiAl grain (Fig. 5). At 1000° C the total strain was

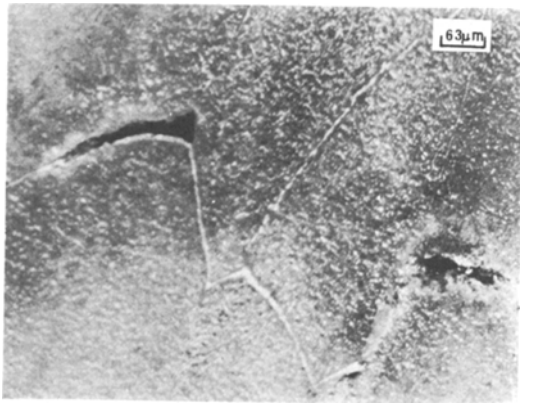

Figure 5 Grain-boundary cavities observed on a specimen deformed to failure at 1000° C and strain rate $\dot{\epsilon} = 10^{-4}$ sec^{-1}.

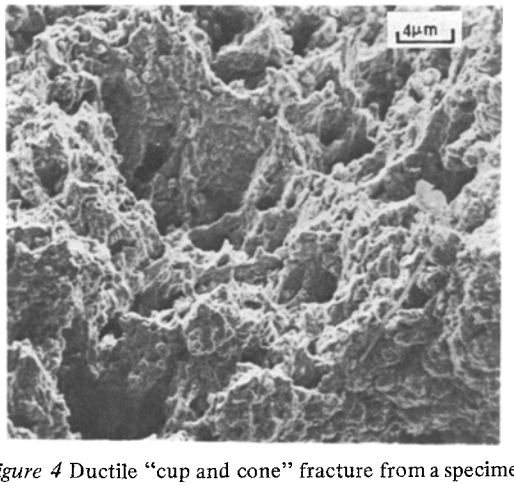

Figure 4 Ductile "cup and cone" fracture from a specimen deformed to failure at 850° C and strain rate $\dot{\epsilon} = 10^{-4}$ sec^{-1}.

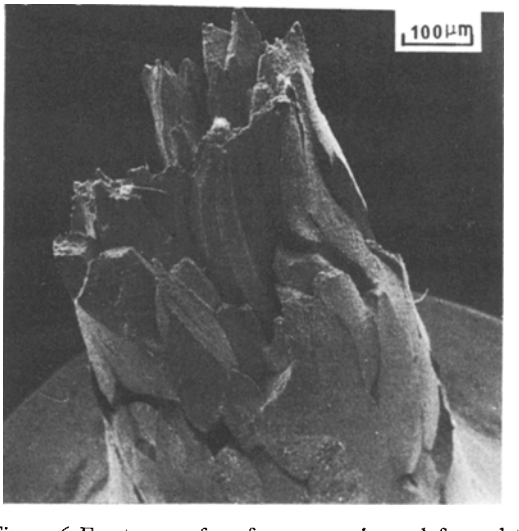

Figure 6 Fracture surface from a specimen deformed to failure at 1000° C and strain rate $\dot{\epsilon} = 10^{-4}$ sec^{-1}.

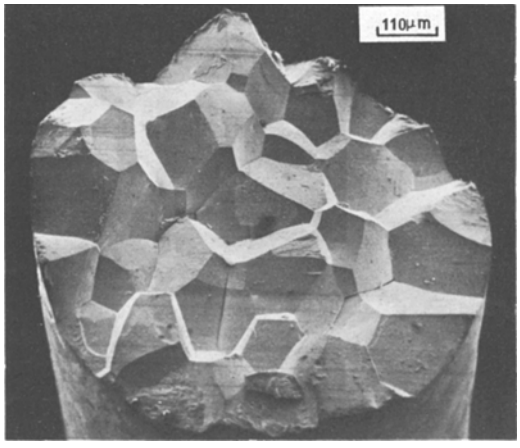

Figure 7 Fracture surface from a specimen deformed to failure at 1000° C and strain rate $\dot{\epsilon} = 10^{-2}$ sec^{-1}.

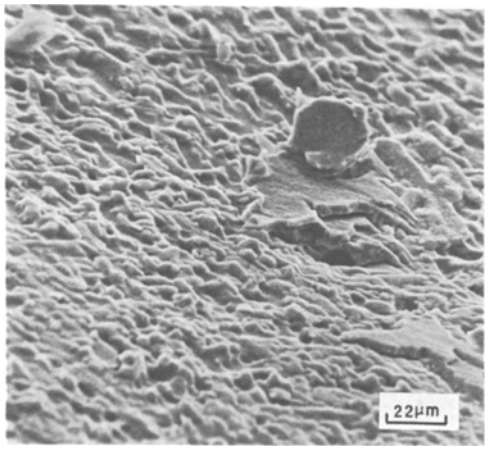

Figure 8 Detailed view of the grain surfaces from the fracture surface in Fig. 7.

accommodated by both grain-boundary sliding and plastic deformation of the grain (see Fig. 6) whilst at 1100° C only massive grain-boundary sliding occurred and grains remained largely undeformed.

The material behaviour at higher strain rate was different. Below 900° C fracture was predominantly cleavage as at lower strain rate, but at 1000° C fracture was entirely intergranular as shown in Fig. 7. Fig. 8 shows the fracture surface at high magnification. The fracture surface is rough, most probably as a result of plastic deformation and ductile failure of the Ni_3Al grain-boundary film.

3.2. Fracture toughness

The value of K_{IC} at room temperature was 50 ± 4 MNm$^{-3/2}$ for the precipitation-hardened condition and 6 ± 0.3 MNm$^{-3/2}$ for the as-quenched martensitic single phase NiAl. These values represent the mean of ten measurements and the error quoted is the standard deviation. The value of K_{IC} for the as-quenched condition is of the same order as that for the engineering ceramic Si_3N_4 and SiC [6]. The value of K_{IC} for the precipitation-hardened condition is approximately half that for cast nickel base alloys such as IN 713 C (100 MNm$^{-3/2}$ [7]).

4. Discussion

The strength of polycrystalline NiAl is temperature dependent. There is a sharp decrease in strength at a homologous temperature of approximately $0.45\,T_m$ [2–4]. Similar behaviour has been observed in the case of two-phase alloy Ni–30.3 at.% Al–6.6 at.% Cr, although in this case the transition temperature increased by 150° C. The mechanism of deformation of polycrystalline NiAl is not very well understood. The operation of the {1 0 0} ⟨0 0 1⟩ and {1 1 0} ⟨1 0 0⟩ slip systems are well established [8–11], but these are not sufficient to provide five independent slip systems for polycrystalline ductility [9]. Dislocations with Burgers vectors $\mathbf{b} = \langle 1\,1\,0 \rangle$ and $\mathbf{b} = \langle 1\,1\,1 \rangle$ were also observed in NiAl [10–13] and if activated they could provide the additional independent slip systems required for polycrystalline ductility. Glide of these dislocations is most likely when zero stress is applied along ⟨1 0 0⟩. However, Fraser *et al.* [14, 15] found that in the temperature range 27° C to 777° C, single crystals of NiAl, compressed along ⟨0 0 1⟩, deformed by movement of dislocations with $\mathbf{b} = \langle 1\,0\,0 \rangle$. These workers showed that glide and climb were competing modes of deformation, where climb was promoted by temperature increases and strain-rate decreases. The behaviour of the two-phase alloy Ni–30.3 at.% Al–6.6 at.% Cr is as expected from the work of Fraser *et al.* [14, 15]. At the lower strain rate the material becomes ductile when the temperature is sufficiently high for climb to accommodate a significant fraction of the strain. Increase in strain rate promotes glide [15] and thus fracture stress is exceeded before enough climb can take place to relieve stresses by plastic deformation.

Two-phase alloy Ni–36 at.% Al appears to be stronger than the present alloy; however, the difference may be due to different experimental techniques used. Russell and Edington [5] used compression techniques and thus were able to measure the flow stress whilst in the present case tensile testing was used and failure may have oc-

curred at stresses below the flow stress of the material.

Russell and Edington showed that the flow stress of the precipitation-strengthened material between 20 and 700° C may be described by the expression:

$$\sigma_y = \sigma_m + \sigma_p \left(\frac{2r_s}{d}\right)^{1/2} \quad (1)$$

where σ_m is the flow stress of the matrix. σ_p is twice the value of the critical resolved shear stress of the Ni_3Al particles, and is regarded as the friction stress of the matrix that must be exceeded to produce plastic flow, r_s is the particle radius, and d the average distance between particles. The validity of this equation can be checked in the present case. The material only exhibited significant tensile strain to failure at the lower strain rate and above 750° C so the results of the calculation are only compared with measurements taken under these conditions. The data which were used in the calculation are tabulated in Table I.

There is no data in the literature giving the values of the flow stresses of the NiAl matrix and the Ni_3Al precipitates for the present compositions. In NiAl with a high supersaturation of Ni, increase in Ni content has little further effect on the value of the flow stress [3], and therefore it is reasonable to assume that σ_m is similar to the flow stress of Ni–41.6 at.% Al [3].

The strength contribution of the grain size can be neglected since the grain-size dependence of the flow stress in NiAl is small [16, 3]. σ_p is assumed to be twice the value of the critical resolved shear stress for $\{0\,0\,1\}\langle 1\,\bar{1}\,0\rangle$ slip, which predominates above 700° C [17] in Ni_3Al and it is quoted by Copley and Kear [18].

The calculated and experimental data are tabulated. Agreement is poor. The discrepancy may be due to the occurence of sliding at the interface between NiAl matrix, Ni_3Al precipitates and grain-boundary film. This phenomenon has been observed at temperatures as low as 700° C during creep of this alloy [19]. It is also in no way certain that the same deformation mechanism operates above 750° C as that below 700° C.

Plastic deformation, during fracture, of Ni_3Al precipitates and Ni_3Al grain-boundary film, and the ability of these precipitates to arrest the crack propagation [5], implies that the particle–matrix interface is strong.

Approximating the present alloy to the fibre-reinforced case, the work done, W, in rupturing the particle is approximately [20]

$$W = YAt \quad (2)$$

where Y is the yield stress of the particle, A is the cross-sectional area, and t the smallest particle dimension. The work done per unit area of the crack surface is then approximately

$$\gamma = \tfrac{1}{2} fYt \quad (3)$$

where f is the volume fraction of the particles. These equations show that a high volume fraction of coarse particles is desirable. Kelly [21] showed that the work of fracture can be increased in two ways in a composite which consists of a brittle matrix strengthened by ductile fibres.

When the matrix fails the load borne by the matrix can be supported by the fibres bridging the plane of fracture of the matrix. The matrix will then fail in another plane and so on, until the matrix will be divided by a series of parallel cracks, lying normal to the axis of the fibres. Kelly [21] estimated that the cracks will be spaced X and $2X$ apart where

$$X = \frac{(1 - V_f)}{V_f} \frac{\sigma_{mu} r}{2\tau_i} \quad (4)$$

where V_f is the volume fraction of fibres, σ_{mu} is the fracture strength of the matrix, r is the radius

TABLE I Data used for the calculation of the flow stress in Equation 1

Temperature (° C)	Volume fraction % Ni_3Al	σ_m (MNm^{-2})	σ_p (MNm^{-2})	Flowstress (MNm^{-2})	
				Calculated	Experimental
755	0.60	93.2	267.8	299.4	450
800	0.52	83.4	276	282.1	146
860	0.52	68.7	248.5	247.6	87
900	0.52	63.8	210	215	59
1000	0.40	38.2	100	101.2	38.7
1100	0.35	14.7	55.2	47.3	15.4

of the fibres and τ_i is the strength of the interface.

Thus the crack length will be controlled by both particle spacing and crack spacing X. The comparison of K_{IC} values for two-phase and single-phase conditions indicates that the presence of Ni_3Al particles must have significantly increased the critical crack size. Thus there can be a considerable subcritical crack growth in two-phase material. This is consistent with the appearance of the fracture surface, observation of stable microcracks [5], and the strain-rate sensitivity of the flow stress. The Ni_3Al phase probably acts in two ways. Firstly stable microcracks can be produced and the crack path in the grains made more complicated. Secondly the grain-boundary Ni_3Al film is likely to reduce the sites for nucleation of cracks if, as has been suggested by Ball and Smallman [9], there is a contribution to crack nucleation from the absence of enough independent slip systems for general ductility.

5. Conclusions

(a) The tensile properties are temperature dependent. Two temperature regions can be distinguished. Below approximately 750° C, the alloy has high strength and low ductility; the temperature and the strain rate have little effect on tensile properties. Above approximately 750° C, there is a rapid decrease of strength and increase of ductility with increasing temperature, and the tensile properties are strain-rate sensitive.

(b) At high strain rate or below 750° C, brittle failure develops which is predominantly transgranular above 900° C. At low strain rate and above 750° C ductile failure develops. There is considerable grain-boundary sliding above 1000° C.

(c) The room temperature fracture toughness is increased in the two-phase material from 6 ± 0.3 $MNm^{-3/2}$ to 50 ± 4 $MNm^{-3/2}$. The fracture toughness is increased because Ni_3Al inhibits the crack nucleation and facilitates the formation of stable microcracks.

Acknowledgements

The author would like to thank Professor J. W. Edington for helpful discussions, Professor R. W. K. Honeycombe for the provision of laboratory facilities, the Ministry of Defence for financial support and International Nickel Limited for supplying the materials.

References

1. E. M. GRALA "Mechanical Properties of Intermetallic Compounds" (ed. J. H. Westbrook) (John Wiley, New York, 1960) p. 358.
2. A. BALL and R. E. SMALLMAN, *Acta Met.* **14** (1966) 1349.
3. R. T. PASCOE and C. W. A. NEWEY, *Metal Sci. J.* **2** (1968) 138.
4. A. G. ROZNER and R. J. WASILEWSKI, *J. Inst. Metals* **94** (1966) 169.
5. K. C. RUSSELL and J. W. EDINGTON, *Metal Sci. J.* **6** (1972) 20.
6. J. W. EDINGTON, D. J. ROWCLIFFE and J. L. HENSHALL, *Powder Metallurgy Internat.* **7** (1975) 82, 136.
7. R. B. SCARLIN, private communication (1975).
8. R. J. WASILEWSKI, S. R. BUTLER and J. E. HANLON, *Trans. Met. Soc. AIME* **234** (1967) 1357.
9. A. BALL and R. E. SMALLMAN, *Acta Met.* **14** (1966) 1517.
10. M. H. LORETTO and R. J. WASILEWSKI, *Phil. Mag.* **23** (1971) 1311.
11. R. T. PASCOE and C. W. A. NEWEY, *Phys. Stat. Sol.* **29** (1968) 357.
12. C. H. LLOYD and M. H. LORRETO, *ibid* **39** (1970) 163.
13. P. R. STRUTT, G. M. ROWE, J. C. INGRAM and Y. H. CHOO, Electron Microscopy and structure of Materials, 1972, University of California press.
14. H. L FRASER, R. E. SMALLMAN and M. H. LORETTO, *Phil. Mag.* **28** (1973) 651.
15. *Idem, ibid.* 667.
16. A. BALL, PhD Thesis, University of Birmingham (1964).
17. P. H. THORTON, R. G. DAVIES and T. L. JOHNSTON, *Met. Trans.* **1** (1970) 207.
18. S. M. COPLEY and B. H. KEAR, *Trans. Met. Soc. AIME* **239** (1967) 977.
19. R. MOSKOVIC, to be published.
20. G. W. GROVES "Strengthening Methods in Crystals" (ed. A. Kelly and R. B. Nicholson) (Elsevier Amsterdam, 1971) ch. 7.
21. A. KELLY, *ibid.* Ch. 8.
22. A. BALL and R. E. SMALLMAN, *Acta Met.* **14** (1966) 1517.

Received 5 July and accepted 15 December 1977.